Doubly-Fed Machine with Wireless Power Transfer Ability

Jun Lee, Jung-Ik Ha
Department of Electrical and Computer Engineering
Seoul National University
Seoul, Korea
leejun1672@snu.ac.kr, jungikha@snu.ac.kr

***Abstract*—In this paper, a current injection method is proposed which enables wireless power transfer in a doubly-fed machine. In the proposed method, currents of the same frequency are injected to both stator current and mover current. The magnitude of the stator side injected current is kept constant during the operation. The mover side injection current is controlled to be in phase with the induced voltage, and the magnitude of the current is used for controlling the voltage of the floating capacitor on the mover. Injection frequency is set higher than the original operation of the machine so that there would be minimal effect on the operation. The proposed method was verified with a simulation, and a position control experiment was performed with an implemented dual-active magnetic bearing system.**

Keywords—Actuation method; self-actuation; wireless power transfer; magnetic actuation

I. INTRODUCTION

An electric machine which has windings on both stator and mover sides has wider operation range and more degree of freedom. A representative system with such structure is doubly-fed induction machine (DFIM). There have been many researches about control and status estimation methods about DFIM [1]–[5]. To utilize the full capability of doubly-fed machines, two independent sources are required for stator and mover. However, it is not easy to supply power to the mover side since an electric wire is needed between the stationary part and moving part. There was a study to operate DFIM using a floating capacitor, but there is a limitation that power cannot be transferred to the rotor under zero torque output [6]. Power transfer around zero torque output might be performed by applying additional control methods such as utilizing negative frequency current, but such solutions still cannot transfer large power over the whole operating range and also accompany huge calculation burden.

To overcome the shortage of doubly-fed machines, a control method which always can deliver power to the mover side should be studied. In this paper, a wireless power transfer based on current injection method is proposed. The currents are injected to both stator and rotor coils, which are used for original operation, so no additional circuit or device is required for power transfer. Injection frequency is set higher than the original operation of the machine so that there would be minimal effect on the operation.

This research was supported by the Korea Evaluation Institute of Industrial Technology funded by the Ministry of Trade, Industry & Energy (10052980).

The proposed current injection power transfer method can be considered as a kind of inductive wireless power transfer. Most of inductive wireless power transfer system works using resonance generated by parallel or series capacitors. However, resonant power transfer method is not applicable for the actuation part of a doubly-fed machine since low frequency force (torque) commands comes to require a large input voltage. Hence, wireless power transfer method only using inductors can be applied.

This paper together proposes a control concept which enables the mover can control the receiving power and actuation force (torque) while stator generates the steady magnetic field. The mover side injection current is controlled to be in phase with the induced voltage, and the magnitude of the current is used for controlling the voltage of the floating capacitor on the mover. With the control method, control burden can be put on the mover side. Also, additional circuits such as communication, power transfer or etc. can be removed from the system. This concept may help designing the control system of a doubly-fed machine.

II. HIGH FREQUENCY INJECTION METHOD FOR WIRELESS POWER TRANSFER IN DOUBLY-FED MACHINE

Since all doubly-fed machines, including rotating machines, can be controlled with DC equivalent circuits in rotating flux reference frame, the proposed method is enough to be verified with the 'dual-active' magnetic bearing system whose references are DC currents in steady state.

'Active' magnetic bearing is composed of a mover at the center and two stators at both sides as shown in Fig. 1(a). The gray areas and yellow areas in Fig. 1 depicts the magnetic material (steel) and coil, respectively. The simplest control of the active magnetic bearing uses bias current and actuation current, which are constant and differential respectively. In such control, current reference can be written as follow.

$$i_{s1} = i_{bias} + i_{act}\,, \quad i_{s2} = i_{bias} - i_{act} \tag{1}$$

Due to the differential current, two air gaps at both ends of the mover comes to have different magnetic field intensity. This leads to the difference of magnetic energy density of two gaps which means that the reluctance forces between the gaps are different from each other. By changing the magnitude and sign

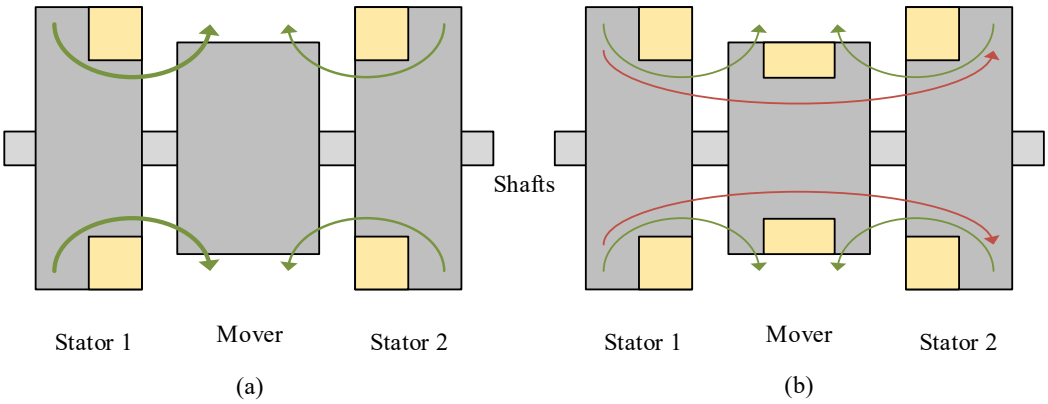

Fig. 1. Structure of (a) stator-only-driven active magnetic bearing and (b) dual-active magnetic bearing.

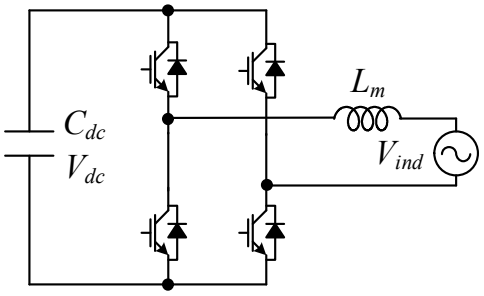

Fig. 2. Mover side equivalent inverter circuit.

of the actuation current, the system can apply a desired force to the mover.

As shown in Fig. 1(b), unlike conventional systems, the mover of the 'dual-active' magnetic bearing has coil on it so that the mover can actuate itself by controlling the current flowing on it. Current references, which actuates the dual-active magnetic bearing system in a similar way to the active magnetic bearing, can be written as follow.

$$i_{s1} = I_{bias} + i_{inj,s}\,, \quad i_{s2} = I_{bias} - i_{inj,s} \tag{2}$$

$$i_m = i_{act} + i_{inj,m} \tag{3}$$

Here, stator side bias current, I_{bias}, has constant value, and mover side actuation current, i_{act}, has low frequency value. The injection currents, $i_{inj,s}$ and $i_{inj,m}$ are sinusoidal currents. Since the injection currents are high frequency sinusoidal currents, the force (torque) generated by these currents does not affect the operation of the machine. The actuation current flowing on the mover side makes the magnetic flux in both ends be different from each other, hence the force applied to the mover is controlled by the mover itself. The actuation property at each position can be pre-investigated with FEM simulation.

If a sinusoidal current with constant magnitude and frequency, $i_{inj,s}\cos(\omega t)$ is injected to the stator, the magnetic field passing through the mover fluctuates. Then, the voltage induced across the mover coil would have the same frequency as $V_{inj}\sin(\omega t)$. Then, the equivalent mover side circuit can be drawn as the inverter circuit with an inductor and sinusoidal voltage source which is shown in Fig. 2. Note that the mover side inverter should control i_{act} and $i_{inj,m}$ at the same time where both currents flow on the same coil. To receive power efficiently, the mover synthesizes sinusoidal voltage or current with the same frequency. Following three power receiving methods can be considered to be applied; they are named as *A*, *B* and *C* methods in this paper. *A* and *B* power receiving methods are voltage injection methods whereas *C* is a current injection method.

A. Maximizing receiving power

By synthesizing the voltage lagging 90° to the voltage induced on the mover coil, V_{inj}, the mover can maximize the receiving power according to the following equation.

$$P = \frac{|V_m||V_{inj}|}{X_m}\sin\theta \tag{4}$$

Here, V_m is the magnitude of the voltage synthesized by the mover side inverter, X_m is the reactance of the mover coil at the injection frequency, and θ is the phase difference between V_m and V_{inj}. If the switching is done in the injection frequency, the theoretical maximum receiving power is

$$P_{max} = -\frac{4}{\pi}\frac{V_{dc}|V_{inj}|}{X_m}\,. \tag{5}$$

By the way, since the inverter is controlling the actuation current at the same time, magnitude of the synthesized voltage, V_m, comes to be smaller than $4V_{dc}/\pi$. So, DC-link voltage should have enough value for both function; receiving power and keeping the force (torque) output. If voltage is not enough, the inverter should concentrate on receiving power rather than force (torque) output, so that the mover can continue the operation. The actuation current controller in this control method does not have to be a PR controller since the injection signal is voltage and can be directly added to the output of the PI current

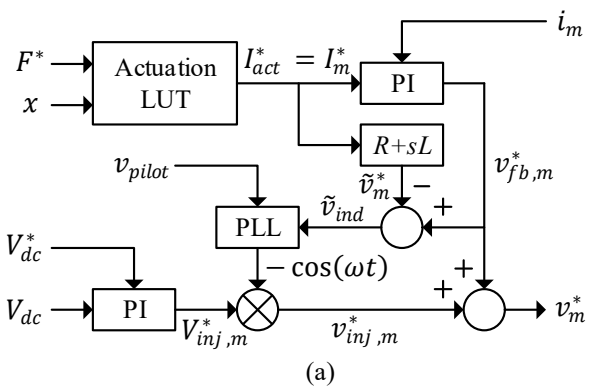

(a)

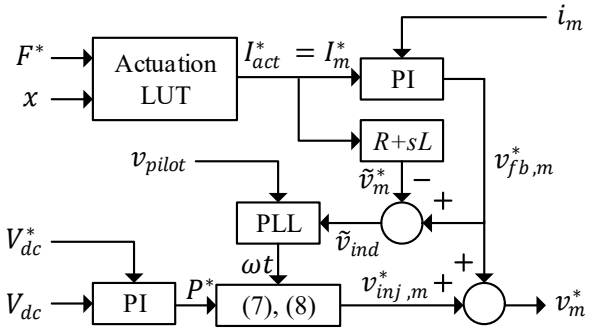

(b)

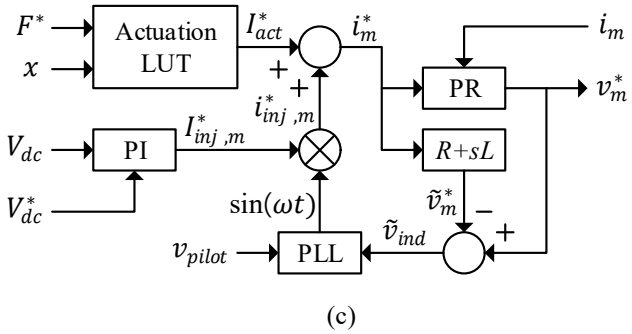

(c)

Fig. 3. Control block diagrams of mover side circuit using different control methods, *A*, *B* and *C*, respectively.

controller. The actuation force (torque) command cannot have high frequency value under this control method because the injected voltage would be compensated with high performance PI controller.

For all control methods, voltage controller can be implemented with PI controller. For the control method *A*, the output of the PI voltage controller becomes the magnitude of the injection voltage. Then, it is injected into the output of the PI current controller, as a sinusoidal voltage having the same frequency with 90° phase delay.

To inject current or voltage to the mover side coil in phase with the induced voltage across it, the controller should know

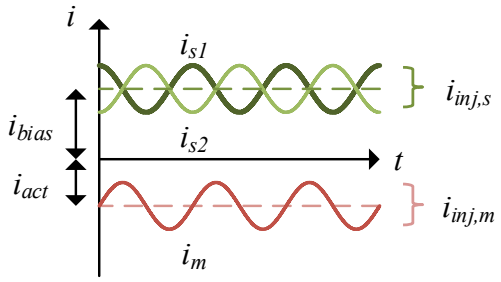

Fig. 4. Stator and mover currents for actuation and power transfer under power receiving method *C*.

the phase (and magnitude) of the induced voltage. The phase can be known by watching the applied voltage by the current controller against the estimated required voltage for synthesizing total mover current, i_m. Or, it can be simply found by using a pilot-coil, which is separately wound on the mover, the phase of the induced voltage can be inferred. The control block diagram of control method *A* is shown in Fig. 3(a).

B. Minimizing ripple of receiving power

Once the DC-link voltage gets enough value, there is no need to concentrate on maximizing the receiving power. So, the goal of the injection control may be changed. It means that the mover side inverter does not have to synthesize voltage with 90° phase delay from the induced voltage across the mover coil.

To minimize the power ripple, reactive power supplied by the 'mover' should be zero; $Q_m = 0$. The magnitude and phase of the mover side injection voltage which makes the mover side reactive power is solved with (4) and (6), and the solution is given as (7) and (8).

$$Q_m = \frac{|V_m|^2}{X_m} - \frac{|V_m||V_{ind}|}{X_m}\cos\theta \tag{6}$$

$$|V_m| = \sqrt{\frac{|V_{ind}|^2 + \sqrt{|V_{ind}|^4 - 4X_m^2P^2}}{2}} \tag{7}$$

$$\theta = \sin^{-1}\left(\frac{X_m P}{|V_m||V_{ind}|}\right) \tag{8}$$

Similar to the control method *A*, a PI current controller should not have high control performance, hence, the actuation force (torque) cannot have high frequency value. Under this method, the output of the PI voltage controller is receiving power, P. Then, injection voltage is decided from (7) and (8) based on the phase and magnitude information (given by PLL) about the induced voltage across the mover side coil. The control block diagram of this power receiving method is shown in Fig. 3(b).

C. Minimizing copper loss

The other control method which minimizes the copper loss actually has a similar approach. The copper loss of the mover side current can be minimized by injecting the current whose magnitude is the smallest value for receiving the required power. Knowing the phase of the induced voltage and given a receiving

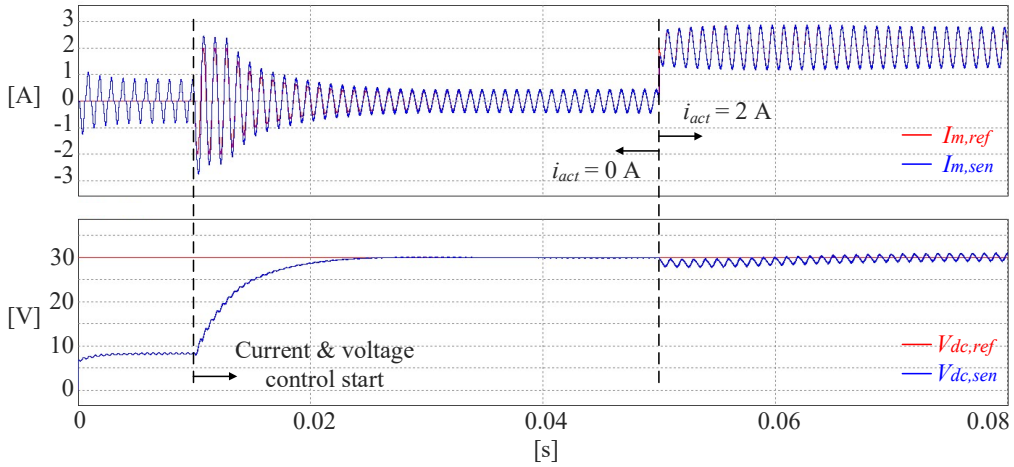

Fig. 6. Simulation result of mover side current and voltage control.

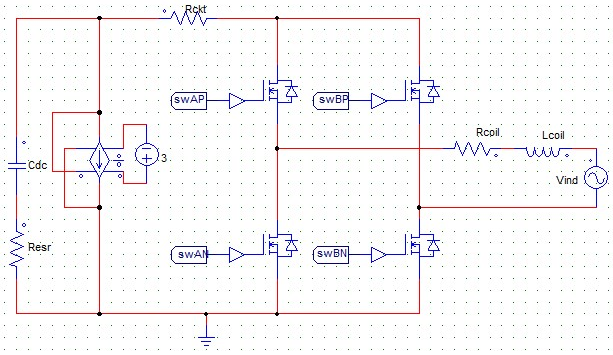

Fig. 5. Simulation circuit of the mover side.

power reference from the voltage controller, the mover inverter can minimize the magnitude of the current by making the current be in phase with the induced voltage. This condition nullify the reactive power supplied by the 'induced voltage'; $Q_{ind} = 0$.

Note that the reactive power supplied by the mover is not zero under this condition. The other way to satisfy this condition is to make the mover current in phase with the induced voltage. Under this control method, the output of the PI becomes the magnitude of the injection current, $I_{inj,m}$, and the injection current in synthesized in phase with the induced voltage. Under this control method, a PR current controller can be applied and enhance the power receiving performance better than a PI current controller. Fig. 3(c) shows the control block diagram of power receiving method C. Stator and mover currents using this method according to time are shown in Fig. 4. In the implemented system, this type of power receiving method was applied.

III. Simulative Verification

To verify whether the mover can control the actuation current and maintain its DC-link voltage at the same time, a simulation was performed. Since the stator side currents are controlled with constant values, steadily, only the mover side equivalent circuit simulated using the circuit shown in Fig. 5. (Controller parts are hidden.) Main values used in the simulation are shown in Table I.

TABLE I. Variables Used in Simulation

Variable	Value	Variable	Value
R_{coil}	0.2 Ω	P_{load}	3 W
L_{coil}	900 μH	R_{ckt}	0.1 Ω
C_{dc}	200 μF	R_{esr}	0.1 Ω
V_{ind}	15 V	f_{sw}	50 kHz
$V_{dc,ref}$	30 V	f_{inj}	1 kHz

Fig. 6 shows the result of the simulation. The power receiving method C explained in the previous section was applied in the simulation. The first graph shows the reference current and sensed current, and the second graph shows the voltage reference and the sensed voltage of the floating DC-link on the mover. The proposed current injection method could control the mover side DC-link voltage and the actuation current simultaneously. It can be seen in the beginning part of the simulation that the magnitude of the injected current is large, and the DC-link voltage gets higher. After DC-link voltage gets to its reference value, the magnitude gets as small as it could handle the power consumed by the load (DSP, switching loss, etc.). When the actuation current becomes 2 A, the resistive loss on the coil and circuit get larger, and this is shown in the result as the increase of the magnitude of the injection current. Since the sinusoidal voltage is induced on the mover side coil, there exists much larger power ripple when the actuation current is not zero.

IV. Experimental Results

Fig. 7 shows the implemented dual-active magnetic bearing system which has the same structure shown in Fig. 1(b). Two stator coils are connected to inverter boards operating with 50

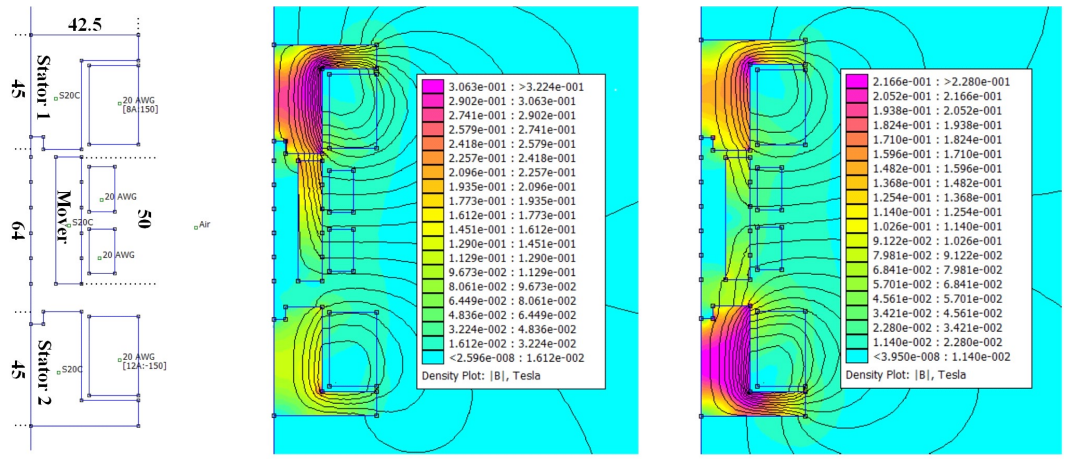

(a) (b) (c)

Fig. 8. (a) FEMM axis-symmetric simulation problem. Feature lengths are written within mm unit. (b), (c) Simulation results (magnetic field density plots) for deciding the number of turns and magnitude of currents.

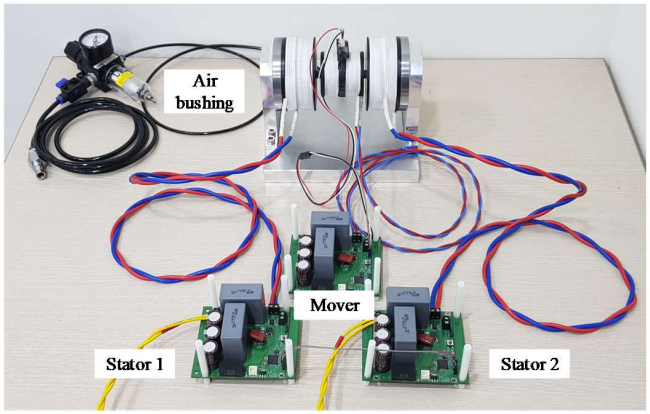

Fig. 7. Implemented dual-active magnetic bearing system.

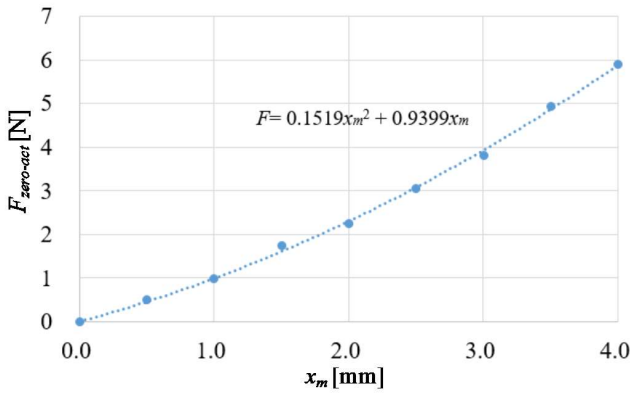

Fig. 9. Pre-investigated zero-actuation-current force.

V DC power supply. Two stator inverter boards were connected with a data cable to synchronize the external magnetic field. Note that the mover coil and its inverter board is completely isolated from the stator. Air bushing is applied to the system to reduce the drag force between the mover and central axis. The position of the mover is measured using an optical sensor which is attached on the mover and connected to the mover side inverter board. Using the FEMM simulation, design parameters in Table II were selected.

TABLE II. PARAMETERS OF IMPLEMENTED SYSTEM

Variable	Value	Variable	Value
N_s	150 turns	I_{bias}	10 A
N_m	40 turns	$I_{inj,s}$	2 A
f_{sw}	50 kHz	$I_{act,\max}$	5 A
f_{inj}	1 kHz	$I_{inj,\max}$	2 A

Variable	Value	Variable	Value
N_s	150 turns	I_{bias}	10 A
L_m	900 µH	C_{dc}	200 µF

Fig. 8 shows the problem and results of the axis-symmetric FEMM simulation of the case when the mover is at 4 mm away from the center. For the result shown in Fig. 8(b), stator currents are set as $i_{s1} = I_{bias} + I_{inj,s} = 12$ A and $i_{s2} = I_{bias} - I_{inj,s} = 8$ A. For the result shown in Fig. 8(c), $i_{s1} = 8$ A and $i_{s2} = 12$ A were used. From these results, the variation of the stator flux passing through the mover can be calculated, hence the number of turns of mover side coil can be decided to get enough induced voltage. After deciding the maximum value of the actuation current, the magnitude of the bias current is decided to apply desired actuation force. Using the FEMM simulation model, induced force at various situation could be known. As the mover moves in the control region, it gets force to the nearer

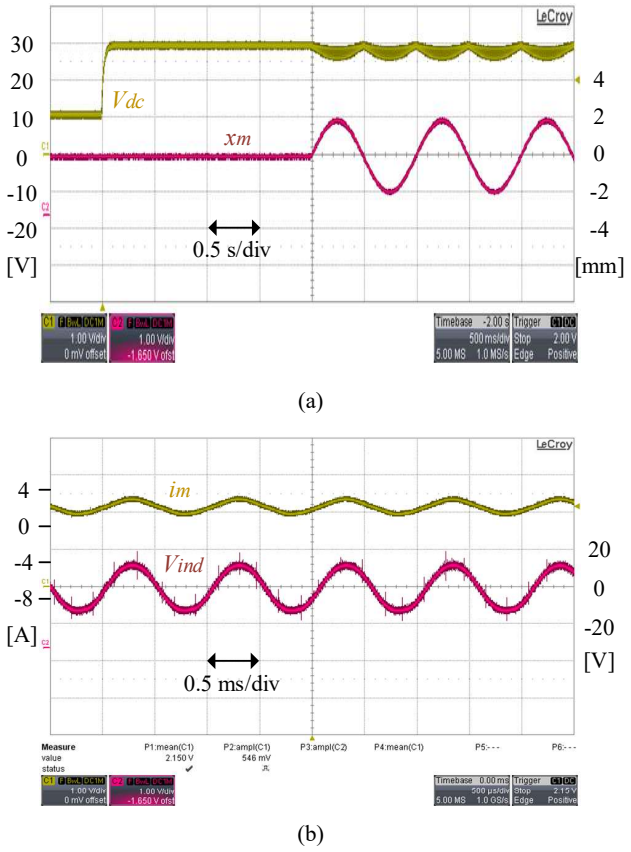

Fig. 10. Experimental results showing (a) the DC-link voltage with the mover position and (b) the mover coil current with the estimated induced voltage. The results show the values stored in the DSP and are measure with the internal D/A converter of the DSP. To see the negative values of the mover position, mover current and induced voltage, the offset of the values are set as 1.65V where the range of the D/A output is 0 to 3.3 V.

stator even if the actuation current is zero due to the magnetic field density difference. The position controller can control the mover better with feedforward term if the zero-actuation-current force according to the mover position is pre-investigated. Fig. 9 shows the pre-investigated zero-actuation-current force graph of the implemented system, and it fit with the second order polynomial very well. A PD controller with the feed-forward table is used for position control, and the position of the mover is measured by the optical sensor attached on the mover. Position-voltage look-up table of the optical sensor was also obtained before starting the experiment. The force induced by unity actuation current changes according to the position of the mover, so it was also pre-investigated using the same FEM model. Actuation coefficient according to the position of the robot also had the second order polynomial form as $F/i_{act} = 0.0247x_m^2 - 0.0194x_m + 0.991$ where units for F, i_{act}, x_m are N, A and mm respectively. So, we can see that three tables (equations) which depend on the position of the mover are used in the system; the zero-actuation-current force, the output voltage of the optical sensor and the actuation coefficient.

Fig. 10 shows the experimental results of the implemented system. (Note that real injected voltage and current would have the switching frequency components but they are not drawn because the D/A conversion was also done within the switching frequency.) Fig. 10(a) shows the implemented system could regulate the DC-link voltage during the position control operation. As expected in the simulation, voltage ripple gets larger as the mover gets nearer to the end of the control region, where the actuation force and current would have the largest values. Fig. 10(b) shows the estimated induced voltage by the mover side current controller and sensed mover side current when the actuation current is at its maximum value. The injected current is controlled to be in phase with the estimated induced voltage. In Fig. 10(b), the magnitude of mover current and induced voltage are about 1.1 A and 14 V, so, it can be inferred that the mover totally consumed about 8 W (at this moment) to control its position while regulating its DC-link voltage. The overall average consumed power by the mover side circuit was about 7 W; note that these values include power for operating DSP and switch driving circuits.

V. CONCLUSION

High frequency injection methods which enable wireless power transfer in the doubly-fed machine are proposed. In the proposed current injection method, the stator synthesizes bias flux and (injected) fluctuating flux which are both steady. Then, the mover can operate itself by controlling the actuation current. Also, the mover can regulate the voltage of floating DC-link capacitor on it by injecting a current in phase with the induced voltage and by changing the magnitude of the injected current. By delivering power through the existing stator and mover coil, there is no need for additional circuit or device, and based on this, the reliability of a doubly-fed machine can be improved.

REFERENCES

[1] J. M. Mauricio, A. E. LeÓn, A. GÓmez-ExpÓsito, and J. A. Solsona, "An Adaptive Nonlinear Controller for DFIM-Based Wind Energy Conversion Systems," *IEEE Trans. Energy Convers*., vol. 23, no. 4, pp. 1025–1035, Dec. 2008.

[2] F. C. Dezza, G. Foglia, M. F. Iacchetti, and R. Perini, "An MRAS Observer for Sensorless DFIM Drives With DirectEstimation of the Torque and Flux Rotor Current Components," *IEEE Trans. Power Electron*., vol. 27, no. 5, pp. 2576–2584, May 2012.

[3] G. D. Marques, D. M. Sousa, and M. F. Iacchetti, "An Open-Loop Sensorless Slip Position Estimator of a DFIM Based on Air-gap Active Power Calculations-Sensitivity Study," *IEEE Trans. Energy Convers*., vol. 28, no. 4, pp. 959–968, Dec. 2013.

[4] A. K. Singh and A. Saxena, "Performance of Sensor and Sensor less Doubly fed Induction motor (DFIM) under the current Sensor fault," in *2016 IEEE 1st International Conference on Power Electronics, Intelligent Control and Energy Systems,* 2016, pp. 1–4.

[5] Y. Han and J. I. Ha, "Control Method of Double Inverter Fed Wound Machine for Minimizing Copper Loss in Maximized Operating Area," *IEEE Trans. Ind. Electron*., vol. PP, no. 99, pp. 1–1, 2017.

[6] K. Lee, Y. Han, and J. I. Ha, "Wound Rotor Machine With Single-Phase Stator and Three-Phase Rotor Windings Controlled by Isolated Three-Phase Inverter," *IEEE Trans. Energy Convers*., vol. 30, no. 2, pp. 558–568, Jun. 2015.